MOLECULAR PHYSICS, 1987, VOL, 62, NO. 5, 1047–1064

High resolution interferometric FTIR spectroscopy of $(HF)_2$: analysis of a low frequency fundamental near 400 cm^{-1}

by K. VON PUTTKAMER and M. QUACK
Laboratorium für Physikalische Chemie der ETH Zürich (Zentrum),
CH-8092 Zürich, Switzerland

(*Received 17 July 1987; accepted 23 July 1987*)

The spectrum of $(HF)_2$ was recorded under equilibrium conditions in a long path thermostated cell at a resolution of 0·02 cm^{-1} between 350 and 550 cm^{-1}.

We present the first rotational analysis of a subband of the low frequency fundamentals of the HF dimer. The subband origins for the two tunnelling components of the $(v = 0, K = 0) \rightarrow (v = 1, K = 1)$ transition were found to be at $400{\cdot}75_{34}$ cm^{-1} (B^+ symmetry in the ground state) and at $399{\cdot}78_{65}$ cm^{-1} (A^+ symmetry in the ground state). The transition is tentatively assigned to the torsional vibration. The tunnelling frequency between the two equivalent isomers of $(HF)_2$ is $48{\cdot}7_7$ GHz for $v = 1$, $K = 1$, about a factor of 1·5 larger than in the ground state ($v = 0$, $K = 1$). The assignment of other subbands is also discussed.

1. Introduction

The dimer of hydrogen fluoride $(HF)_2$ is one of the simplest prototype molecules with hydrogen bonding [1]. Understanding its structure and dynamics will provide insight into detailed aspects of hydrogen bonding, which is important for a wide range of phenomena covering the structure of hydrogen bound liquids and their kinetics of evaporation and condensation, biological primary processes related to hydrogen bonding [1] and collisional energy transfer processes, say in the HF laser [2]. $(HF)_2$ has thus already been the subject of a variety of spectroscopic studies [3–17], including the vapour phase equilibria [18] and numerous theoretical studies of the potential energy surface [19–24].

From the pioneering studies in microwave spectroscopy [3–6] one knows that $(HF)_2$ is a planar, slightly asymmetric top with a nearly linear hydrogen bond and an average F–H···F distance of about 278 pm. The non H-bonded H atom is bent 63° off the F···F axis and executes a large amplitude exchange with the H-bonded H-atom leading to a tunnelling splitting of 0·6587 cm^{-1} in the vibrational ground state ($K = 0$, for $K = 1$: 1·064 cm^{-1}). The $(HF)_2$ molecule is thus also an interesting example for the application of non-rigid molecule group theory [25–29].

The high frequency HF stretching vibrations have been studied by Pine *et al.* [8, 9] at high resolution allowing both the rotational analysis and the determination of the predissociation linewidths, which are significantly mode dependent [8, 9] thus indicating mode selective predissociation behaviour [30]. We have been able to demonstrate that relatively narrow line structure is also visible in the HF stretching overtone spectrum of $(HF)_2$ [10, 11].

A careful search of the literature indicated a complete lack of high resolution analyses of the low frequency fundamentals of $(HF)_2$. These low frequency funda-

mentals are, however, of crucial importance for understanding both the potential surface for hydrogen bonding at large amplitudes of motion and for more detailed investigations of the predissociation dynamics. We thus started, some time ago [10, 11] a systematic investigation of the far infrared spectrum of $(HF)_2$. The present paper provides the first detailed account of the rovibrational analysis of a band near $400\,cm^{-1}$, which is tentatively assigned to the torsional fundamental transition.

2. Experimental

The spectra have been recorded between 350 and $550\,cm^{-1}$ on our BOMEM DA 002 interferometric Fourier transform spectrometer system allowing for a maximum resolving power of about 10^6 (apodized bandwidth $0{\cdot}004\,cm^{-1}$). The spectra analysed below have been taken with an instrumental bandwidth of $0{\cdot}02\,cm^{-1}$, optimizing the signal to noise ratio also in relation to pressure broadening. We used a home built thermostated stainless steel cell with transfer optics giving an optical path length of 10 m. $(HF)_2$ was created under equilibrium conditions between 250 K and 300 K at total pressures between 2 and 10 k Pa. The temperature was controlled to about ± 1 K. The signal strengths could be correlated with the approximately known $(HF)_2$ partial pressures from the equilibrium constant. Unambiguous identification of the dimer spectrum is also available by means of combination differences (see below). HF was obtained from Matheson. There were no appreciable impurities other than small amounts of air and water. Some of our spectra showed the SiF_4 absorption near $389\,cm^{-1}$. This is probably due to the reaction of HF with Si-impurities in the polyethylene windows of the cell. The frequencies were calibrated against known frequencies for the HF monomer and for water [40]. The corrections were always small.

3. Results and discussion

3.1. *The I.R.-spectrum of gaseous hydrogen fluoride between 350 and 550 cm^{-1}*

Under equilibrium conditions the far infrared spectrum of hydrogen fluoride shows the prominent lines of the pure rotational spectrum of HF, extending to high frequencies, and in addition extended bands with very complex fine structure (looking like 'noise') and some broad background, which is difficult to distinguish from artifacts. Figure 1 shows a low resolution overview of the region between 395 and $505\,cm^{-1}$. The strongest feature assigned to $(HF)_2$ appears at the low frequency end of the spectrum near $400\,cm^{-1}$, with structures extending to both low and high wavenumbers. As shown by the detailed assignment in figure 2, which is discussed below, this feature can be clearly assigned to $(HF)_2$ with two strong Q-branches and subband origins at $400{\cdot}75_{34}\,cm^{-1}$ and $399{\cdot}78_{65}\,cm^{-1}$. Further, weaker bands can be identified by band heads near $432{\cdot}2\,cm^{-1}$, $451{\cdot}3\,cm^{-1}$ and $471{\cdot}9\,cm^{-1}$. Even without detailed rotational assignments these can be identified as $(HF)_2$ absorptions, because of their pressure and temperature dependence. In contrast to this the obvious band with a maximum near $500{\cdot}14\,cm^{-1}$ shows different pressure and temperature dependences as well as some other weak and unstructured absorptions, which are perhaps due to higher $(HF)_n$ polymers.

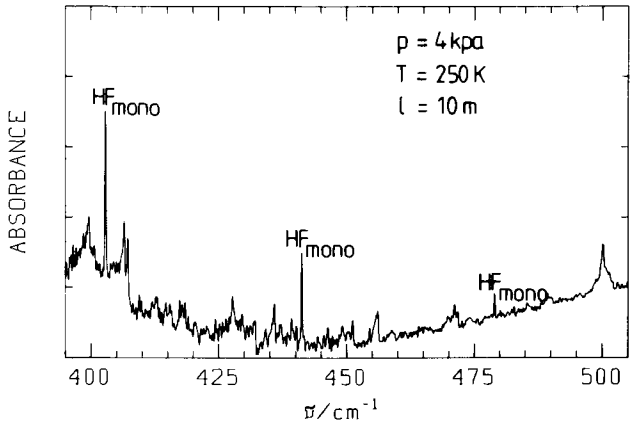

Figure 1. Low resolution ($0{\cdot}3\,cm^{-1}$) survey spectrum of gaseous hydrogen fluoride, $p = 4\,kPa$, $l = 10\,m$, $T = 250\,K$. HF_{mono} indicates monomer rotational lines.

To low wavenumbers there is another intense band with Q-branch centres at $383{\cdot}34_4$ and $382{\cdot}02_8\,cm^{-1}$. The R-branch regions of these bands overlap with P and Q-branch transitions of the band at $400\,cm^{-1}$ and are thus very congested and difficult to analyse. Before discussing the detailed rovibrational assignment, we shall summarize the current knowledge about the expected vibrational transitions at low frequencies of $(HF)_2$.

3.2 *Preliminary discussion of the vibrational assignment*

For the $(HF)_2$ molecule one has six vibrational fundamentals, five of A' species in the C_s point group and one of A'' species in C_s (out-of-plane bending, hereafter called torsion). Two of the high frequency fundamentals are essentially HF stretching vibrations, which have been well studied [8, 9]. None of the low frequency vibrations has so far been analysed in detail. Table 1 summarizes theoretical predictions and table 2 some absorptions observed in low temperature matrix spectros-

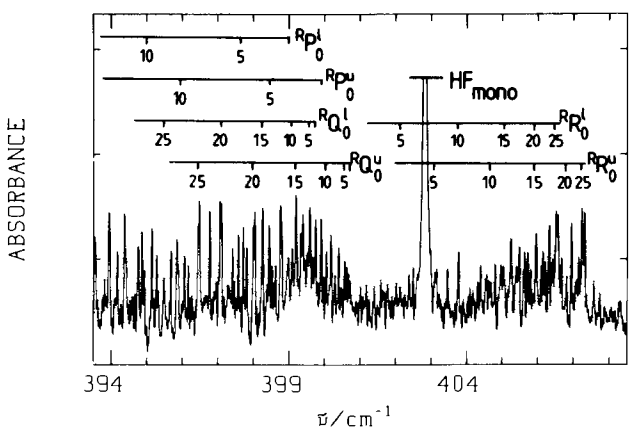

Figure 2. The $K = 1 \leftarrow 0$ torsional subband of the $(HF)_2$ molecule (resolution $0{\cdot}02\,cm^{-1}$ FWHM, apodized) $p = 2\,kPa$, $T = 250\,K$, $l = 10\,m$.

Table 1. Predicted§ and observed fundamental frequencies of $(HF)_2$.

$\tilde{\nu}/cm^{-1}$						
$\nu_1(A')$	$\nu_2(A')$	$\nu_3(A')$	$\nu_4(A')$	$\nu_5(A')$	$\nu_6(A'')$	Reference and level of calculation
4279	4242	551	221	154	463	[19], HF/6–31
3905	3852	607	243	174	497	[19], MP2/6–31
4127	4054	582	231	163	516	[19], MP2/6–311
4070	4021	519	189	165	475	[20], DZ/SCF
3773	3743	523	196	166	459	[20], DZ/CI
4153	4095	607	218	156	486	[20], DZ + P/CI
4081	4038	588	226	171	519	[21], LCAO/SCF
3873	3753	697	333	212	623	[14], (H3)
3976¶	3920¶	420§	127§	157¶	—	[41]
—	—	520	178	337	same order	[23]‖
—	—	304	148	160	as ν_3	[23]¶
3930·903†	3868·313†	—	—	—	$399{\cdot}78_{65}$ ‡	[9]†, this work‡
3930·459†	3867·421†	—	—	—	$400{\cdot}75_{34}$ ‡	[9]†, this work‡

† Ref. [9], upper line is for the symmetric tunnelling component in the ground state, the lower line for the antisymmetric component. Both are for the $K' = K'' = 0$ state.

‡ This work, with the preliminary assignment to torsion, upper line for symmetric tunnelling component in the ground state, lower line for antisymmetric one. Both are assigned to the $K' = 1$, $K'' = 0$ state.

§ The predicted frequencies are mostly uncorrected for anharmonicity.

‖ Uncorrected for anharmonicity, from a semiempirical potential surface model.

¶ Corrected for anharmonicity.

copy. The four low frequency fundamentals can be grouped in a high frequency pair, predicted to fall between $300\,cm^{-1}$ to $700\,cm^{-1}$ (at most) and a low frequency pair, about 150 to $300\,cm^{-1}$. The A'' torsion is predicted to belong to the high frequency pair. The matrix spectra show absorptions at a number of frequencies in this range. The band at $400\,cm^{-1}$ could thus be due either to the torsional ν_6 or to the high frequency in plane bending fundamental ν_3. There are also, in principle, three possible overtone and combination transitions from the low frequency fundamentals that may fall in this frequency range. Two of these would involve excitation of the large amplitude bending vibration ν_5 with much increased tunnelling splitting, which we exclude below. The third would be the overtone $2\nu_4$ of the dimer stretching vibration. This coordinate corresponds to dissociation along the F–H···F axis, with a dissociation wavenumber of about $1600\,cm^{-1}$.

Table 2. Absorptions assigned to the $(HF)_2$ molecule in low resolution vapour phase spectroscopy and low temperature matrix spectroscopy.

Wavenumber/cm^{-1}				Remarks [ref.]
	381			Vapour [13]
	385			Vapour [12]
561	446; 400			Ar matrix [14]
	400		189	Ar matrix [16]
		263		Ar matrix [17]
523	441			CO matrix [14]
	410			Ne matrix [15]

Further evidence for the assignment arises from the rotational polarization of the transition. The in plane vibrations are A/B hybrids, whereas the torsion is of type C [32]. With an asymmetry parameter $\kappa \simeq -0{\cdot}998$, we can use essentially symmetric top selection rules. The hydrogen bond stretching vibration and its overtones are polarized along the top axis, leading to parallel bands with weak Q-branches because of the very large A rotational constant and the low $K_a \equiv K$ quantum numbers contributing to the spectrum. All other low frequency fundamentals give rise to perpendicular bands with a wide K structure and strong Q-branches in the K subbands. The observed structure roughly matches a perpendicular like transition and would thus have to be assigned either to the torsional (A'', ν_6) or to the high frequency in plane bending vibration (A', ν_3). The temperature dependent measurements do not indicate the possibility of a vibrational hot band transition for the dominant part of the spectrum.

3.3. *Detailed rotational analysis*

The $(HF)_2$ molecule is highly non rigid with large amplitude motions both by vibration and by rotation. This has consequences, which have been discussed before [3–9, 29] and will be outlined here briefly, in order to make the analysis and notation comprehensible. $(HF)_2$ exists in two equivalent planar conformations which may easily interconvert as shown in figure 3. The tunnelling splittings related to this interconversion are easily observed, of the order of $1\,\mathrm{cm}^{-1}$, depending strongly on the rotational and vibrational state [3–9]. The molecular symmetry group [25] is of order 4 and its character table is given in table 3. $(HF)_2$ is planar and the group is thus the direct product of the space inversion group $S^* = \{E, E^*\}$ and the permutation group involving the interchange of the two HF units a and b, $\{E, (ab)\} \equiv \{E, (13)(24)\}$. We use the systematic notation of [26] indicating parity ($\pm$) explicitly in the symbols for the species. The relationship to the C_{2h} point group notation [29] related to the most probable trans-tunnelling path originally suggested by Mills is given in parentheses. Each A^+ (A') or A^- (A'') level in C_s symmetry is split by tunnelling in a $(A, B)^+$ and $(A, B)^-$ pair. The optical electric dipole selection rules are

(i) parity change ($+ \leftrightarrow -$); and

(ii) conservation of nuclear spin symmetry (i.e. $A \not\leftrightarrow B$).

Figure 4 is a diagram which shows (for the band observed here) the tunnelling splittings, symmetry species, optical transitions and nuclear spin statistical weights, which are easily obtained from elementary considerations in this simple symmetry

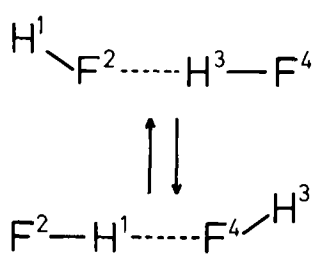

Figure 3. Scheme of $(HF)_2$ conformations and interconversions—definition of the numbering of the nuclei for the molecular symmetry group.

Table 3. (*a*) Character table for the molecular symmetry group M_{S4} of $(HF)_2$.

Species	E	E^*	(ab) (13)(24)	$(ab)^*$ (13)(24)*	$(M_{S4}) \uparrow S^*_{2,2}$
$A^+ (A_g)$	1	1	1	1	$A_1^+ + A_2^+$
$A^- (A_u)$	1	−1	1	−1	$A_1^- + A_2^-$
$B^+ (B_u)$	1	1	−1	−1	$B_1^+ + B_2^+$
$B^- (B_g)$	1	−1	−1	1	$B_1^- + B_2^-$

(*b*) Character table for $S_{2,2}$.

Species	E	(13)	(24)	(13)(34)	$(S_{2,2}) \downarrow M_{S2}$
$A \times A \equiv A_1$	1	1	1	1	A
$B \times B \equiv A_2$	1	−1	−1	1	A
$B \times A \equiv B_1$	1	−1	1	−1	B
$A \times B \equiv B_2$	1	1	−1	−1	B

group. The symmetric (A) nuclear spin functions combining with the A motional functions may have total nuclear spin $I = 2$, 1 or 0 (twice for the latter, total weight $g = 10$) and the antisymmetric (B) nuclear spin functions, combining with B levels, may have $I = 1$ (twice, total weight $g = 6$). Table 3 shows for completeness also the induced representations $\Gamma(M_{S4}) \uparrow S^*_{2,2}$ for the full permutation inversion group.

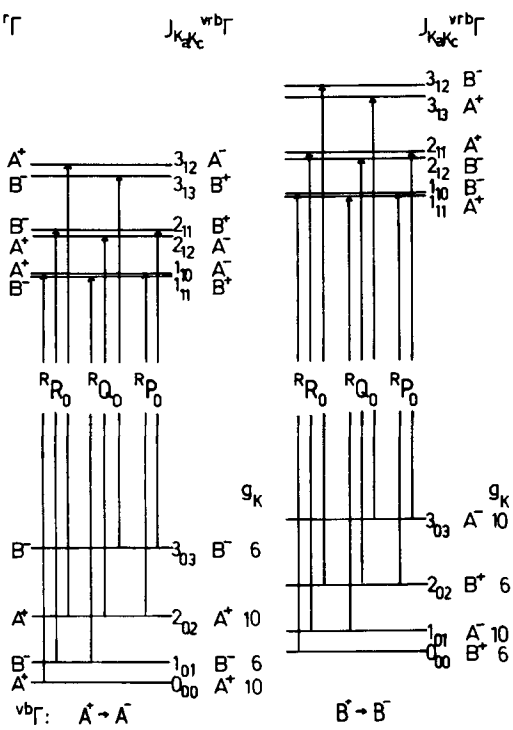

Figure 4. Scheme for the observed rovibrational transitions assigned to the torsional fundamental of $(HF)_2$ $\Gamma^{vb}\Gamma^r = \Gamma^{vrb}$ is the vibrational, rotational species *including* the bending motion with the tunneling splitting. Γ^r is the rotational species.

Only the character table for $S_{2,2}$ is defined and parity is simply to be added. The splittings in these doublets $A_1 + A_2$ and $B_1 + B_2$ with either + or − parity are related to the tunnelling, if proton transfer across the hydrogen bond and consequently also of the second proton were to become important. No such splittings have been observed to date and they are estimated to be quite small. One might speculate that the splitting may become appreciable at very high overtones for the HF stretching vibration, but we have found no evidence for this [33]. These considerations define thus the level structure arising from tunnelling.

The second pecularity due to large amplitude motion arises from the rotation around the symmetric top a-axis (about F···H-F line), which has an extremely large rotational 'constant' A and centrifugal perturbation as is obvious already from chemical intuition. As discussed in detail by Pine *et al.* [8, 9] it is best to treat every $K = K_a$ level with an independent set of constants and the approximate term formula

$$\frac{E_{vK}}{hc} = \tilde{\nu}_{vK} + \bar{B}_{vK} J(J+1) - D_{vK}[J(J+1) - K^2]^2 + \frac{\Delta E_{vK}}{hc}, \tag{1 a}$$

$$\frac{\Delta E_{vK}}{hc} = \pm\delta_{K1}[\tfrac{1}{4}(B_{vK} - C_{vK})J(J+1) + \tfrac{1}{2}l_{vK} J^2(J+1)^2]. \tag{1 b}$$

$\tilde{\nu}_{vK}$ is the subband origin of the K transition and $\bar{B}_{vK} = (B_{vK} + C_{vK})/2$ is the average rotational constant. E_{vK} is a near symmetric top approximation with an asymmetry splitting ΔE_{vK}, which is appreciable only for $K = 1$ (Kronecker delta δ_{K1} in equation (1 *b*)). The + sign in equation (1 *b*) corresponds to $K_a + K_c = J$ and the − sign to $K_a + K_c = J + 1$. D_{vK} and l_{vK} are the appropriate centrifugal constants. Higher order corrections could be neglected in our fits. These fits were extended to values of $J'' = 31$, converging well, using the Marquardt algorithm [34].

Table 4 summarizes the lines which could be assigned to the first tunnelling component with a subband origin at $400{\cdot}75_{34}\,\mathrm{cm}^{-1}$. The values in parentheses are of lines broadened by overlapping with other lines or are otherwise uncertain and were not used in the fit. The J-assignment is quite well established. When fitting the Q- and R-branches separately we obtained with the J-assignment of table 4 the same subband origin for both fits within the standard deviation (about a tenth of the resolution). A change of the J-assignment by ± 1 for the Q-branch leads to a discrepancy by about twice the resolution, i.e. a factor of 20 poorer, which is significant. The lowest J'', which could be assigned is 2, lower values leading to weak and overlapping bands. Lines with odd J'' are more intense. This identifies the assignment of the vibronic symmetry of the lower state of the transition as $\Gamma^{vb''} = B^+$ (we write Γ^{vb} in order to specify vibronic symmetry species including the bending motion giving the tunnelling splitting using M_{S4}, see also [29]). From combination differences we can establish that the lower vibrational state of the transition is the vibrational ground state (except for the tunnelling splitting)

$$\Delta_2 F(J''_{K_aK_c}) = F''(J+1) - F''(J-1) = R(J-1) - P(J+1). \tag{2}$$

These values are summarized in table 5 and are compared with accurate data from microwave [3–6] and near-IR laser spectroscopy [8, 9]. The root mean square deviation for the best assignment is about 20 per cent of the resolution. An accidental agreement with rotational levels from an excited vibrational state (except for tunnelling) can be safely excluded at this level. The rotational K assignment can also

Table 4. Assigned transitions of the band with subband origin at $400{\cdot}75_{34}\,\mathrm{cm}^{-1}$ (values in parentheses were not included in the fit). The ground level constants were fixed in the fit. The root mean square deviation is $0{\cdot}004\,\mathrm{cm}^{-1}$ for 51 lines with 5 parameters. (The wavenumbers are all calibrated and corrected.)

		Wavenumber/cm^{-1}	
J'	J''	$\tilde{\nu}_{\mathrm{exp}}$	$(\tilde{\nu}_{\mathrm{exp}} - \tilde{\nu}_{\mathrm{calc}})$
5	6	(397·965)	−0·0068
6	7	(397·461)	−0·0047
9	10	(395·871)	−0·0026
10	11	395·3182	0·0000
11	12	394·7519	0·0016
12	13	394·1665	−0·0033
13	14	(393·550)	−0·0266
14	15	(392·956)	−0·0145
16	17	391·7107	−0·0084
17	18	391·0769	0·0034
18	19	390·4143	0·0000
19	20	389·7494	0·0080
20	21	389·0511	−0·0034
22	23	387·6438	0·0059
23	24	386·9050	−0·0026
24	25	(386·175)	0·0126
26	27	(384·617)	−0·0088
27	28	383·8380	0·0042
28	29	383·0208	−0·0048
29	30	(382·184)	−0·0168
2	2	(400·721)	0·0060
3	3	400·6727	−0·0038
4	4	400·6283	0·0031
5	5	400·5639	0·0028
6	6	400·4780	−0·0059
7	7	400·3961	0·0023
8	8	400·2914	0·0009
9	9	400·1743	0·0001
10	10	400·0443	−0·0002
11	11	399·9013	−0·0002
12	12	399·7415	−0·0036
13	13	399·5794	0·0043
14	14	399·3851	−0·0063
15	15	399·1927	−0·0011
16	16	(398·978)	−0·0042
17	17	398·7596	0·0031
18	18	398·5176	0·0012
19	19	398·2561	−0·0057
20	20	397·9959	0·0034
21	21	397·7085	0·0002
22	22	397·4073	−0·0017
23	23	397·0974	0·0030
24	24	396·7696	0·0054
25	25	(396·414)	−0·0042
26	26	396·0513	−0·0048
27	27	(395·671)	−0·0068
28	28	(395·274)	−0·0088
29	29	(394·856)	−0·0150

Table 4 (*continued*).

		Wavenumber/cm^{-1}	
J'	J''	$\tilde{\nu}_{exp}$	$(\tilde{\nu}_{exp} - \tilde{\nu}_{calc})$
4	3	402·3656	0·0030
6	5	403·0969	0·0049
7	6	403·4454	0·0079
8	7	403·7654	−0·0046
9	8	404·0943	0·0050
10	9	(404·389)	−0·0063
11	10	404·6830	−0·0048
12	11	404·9628	−0·0037
13	12	(405·244)	0·0130
14	13	405·4776	−0·0043
15	14	405·7171	−0·0009
16	15	(405·952)	0·0129
17	16	406·1437	−0·0023
18	17	(406·327)	−0·0100
19	18	406·5143	0·0013
20	19	406·6704	−0·0024
21	20	406·8122	−0·0042
22	21	406·9454	0·0019
23	22	407·0613	0·0076
24	23	407·1488	0·0023
25	24	(407·235)	0·0135
26	25	(407·267)	−0·0119
27	26	(407·314)	−0·0035

be established on the basis of our data. $K > 2$ can be excluded at once because of the assigned $J'' = 2$. K doubling is not observed, although it might possibly occur for a $K = 1 \leftarrow 2$ transition. The observation of intensity alternation excludes $K_a \geqslant 2$ because K_c = even or odd are not split appreciably for these K_a. Hence, only $K = 0$ or 1 need be considered. Table 5 gives root mean square deviation for various K assignments. It is evident that only $K'' = 0$ is consistent with the data. The assignment of the tunnelling components of the vibrational ground level is somewhat less obvious from the frequency data alone.

Table 6 gives the assigned transitions for the second tunnelling component with a subband origin at $399{\cdot}78_{65}\,\mathrm{cm}^{-1}$. Here, especially the Q-branch transitions from the lower J'' overlap with transitions of the $400{\cdot}75_{54}$ band. Using nuclear spin statistics and the other procedures discussed above, we conclude that the band is a transition from $K'' = 0$ in the ground state to $K' = 1$ in the excited state. Q-branch transitions go to the lower, P and R-branch transitions to the upper level of the asymmetry split $K_a = 1$ vibrationally excited state. This is true for both subbands and is illustrated in figure 4. Nuclear spin statistics establish the vibronic species of the lower state to be $\Gamma^{vb''} = A^+$.

Table 7 summarizes the spectroscopic constants obtained from the fits for the two subbands. Figure 5 shows a detail of the comparison of the experimental and simulated spectrum. Noting that some congestion from weak hot band transitions is expected, the agreement is very good.

Table 5. Ground state combination differences $\Delta_2 F''(J)$ (see also text).

	$\Delta_2 F''/\mathrm{cm}^{-1}$								
			Microwave data§						
J	$\Delta_2 F''(J)$†	$\Delta_2 F''(J)$‡	$J_{K_aK_c}$	$\Delta_2 F''(J)$ A^+	$\Delta_2 F''(J)$ B^+	$J_{K_aK_c}$	$\Delta_2 F''(J)$ A^+	$J_{K_aK_c}$	$\Delta_2 F''(J)$ A^+
10	9·0793		$10_{0\,10}$	9·0825	9·0771	$10_{1\,10}$	9·0995	$10_{1\,9}$	9·1654
11		9·9311	$11_{0\,11}$	9·9433	9·9374	$11_{1\,11}$	9·9621	$11_{1\,10}$	10·0340
12		10·7963	$12_{0\,12}$	10·8030	10·7965	$12_{1\,12}$	10·8235	$12_{1\,11}$	10·9015
15	13·3752		$15_{0\,15}$	13·3741	13·3662	$15_{1\,15}$	13·4000	$15_{1\,14}$	13·4960
17	15·0735	15·0668	$17_{0\,17}$	15·0804	15·0717	$17_{1\,17}$	15·1103	$17_{1\,16}$	15·2179
19		16·7649	$19_{0\,19}$	16·7797	16·7702	$19_{1\,19}$	16·8136	$19_{1\,18}$	16·9326
20	17·6276	17·6193	$20_{0\,20}$	17·6263	17·6165	$20_{1\,20}$	17·6624	$20_{1\,19}$	17·7871
21	18·4613		$21_{0\,21}$	18·4709	18·4607	$21_{1\,21}$	18·5092	$21_{1\,20}$	18·6394
22	19·3173	19·3016	$22_{0\,22}$	19·3132	19·3027	$22_{1\,22}$	19·3543	$22_{1\,21}$	19·4894
23	20·1503	20·1563	$23_{0\,23}$	20·1532	20·1424	$23_{1\,23}$	20·1962	$23_{1\,22}$	20·3371
25	21·8324		$25_{0\,25}$	21·8257	21·8144	$25_{1\,25}$	21·8737	$25_{1\,24}$	22·0251
27		23·4760	$27_{0\,27}$	23·4875	23·4758	$27_{1\,27}$	23·5408	$27_{1\,26}$	23·7023
rms‖:	$\tilde{\nu} = 399{,}7865\,\mathrm{cm}^{-1}$			0·0053	0·010		0·0372		0·1588
	$\tilde{\nu} = 400{,}7534\,\mathrm{cm}^{-1}$			0·0107	0·0061		0·0453		0·1658

† For the band with subband centre at $399{\cdot}7865\,\mathrm{cm}^{-1}$.
‡ For the band with subband centre at $400{\cdot}7534\,\mathrm{cm}^{-1}$.
§ From [3, 4, 5, 8, 9].
‖ The root mean square deviation is given for possible assignments of the subbands to different transitions as indicated. $\mathrm{rms}^2 = N^{-1}\sum_{i=1}^{N}(\Delta_2 F''_i - \Delta_2 F''_{i\,(\mathrm{microwave})})^2$. N = number of assigned differences.

Table 6. Assigned transitions of the band with subband origin at $399{\cdot}78_{65}\,\mathrm{cm}^{-1}$. The root mean square deviation for 43 lines and 5 parameters is $0{\cdot}0031\,\mathrm{cm}^{-1}$ (see also table 4).

		Wavenumber/cm^{-1}	
J'	J''	$\tilde{\nu}_{\mathrm{exp}}$	$(\tilde{\nu}_{\mathrm{exp}} - \tilde{\nu}_{\mathrm{calc}})$
8	9	(395·477)	0·0162
9	10	394·924	0·0030
10	11	394·3661	−0·0032
11	12	393·8100	0·0044
12	13	393·2269	−0·0029
13	14	(392·637)	−0·0048
15	16	391·4286	−0·0002
16	17	(390·806)	0·0025
17	18	390·1708	0·0052
20	21	388·1758	0·0018
21	22	387·4911	0·0074
22	23	386·7798	0·0000
23	24	386·0637	0·0016
24	25	(385·342)	0·0116
25	26	384·5833	−0·0011
26	27	(383·840)	0·0161
27	28	(383·045)	−0·0037

Table 6 (*continued*).

		Wavenumber/cm^{-1}	
J'	J''	$\tilde{\nu}_{exp}$	$(\tilde{\nu}_{exp} - \tilde{\nu}_{calc})$
2	2	(399·743)	−0·0055
4	4	(399·662)	0·0023
5	5	(399·584)	−0·0122
6	6	(399·531)	0·0111
7	7	(399·432)	0·0016
8	8	399·3263	−0·0022
9	9	(399·219)	0·0057
10	10	399·0863	0·0014
11	11	(398·956)	0·0126
12	12	398·7860	−0·0025
13	13	398·6188	−0·0013
14	14	398·4429	0·0047
15	15	(398·256)	0·0137
16	16	398·0333	0·0005
17	17	397·8053	−0·0039
18	18	397·5671	−0·0042
20	20	397·0550	0·0029
21	21	396·7696	−0·0007
22	22	396·4732	−0·0004
23	23	396·1630	0·0015
24	24	395·8385	0·0045
25	25	(395·473)	−0·0175
26	26	395·1329	0·0014
27	27	394·7519	−0·0041
28	28	(394·366)	0·0021
29	29	(393·938)	−0·0170
30	30	(393·529)	0·0000
31	31	(393·071)	−0·0145
3	2	(401·014)	−0·0011
4	3	401·4001	−0·0004
5	4	401·7767	0·0031
6	5	(402·121)	−0·0135
7	6	402·4864	0·0035
9	8	403·1439	0·0022
10	9	403·4454	−0·0065
11	10	(403·765)	0·0163
13	12	404·3008	−0·0027
14	13	404·5608	0·0005
15	14	404·8038	0·0005
16	15	405·0285	−0·0038
17	16	405·2443	−0·0026
19	18	405·6313	−0·0009
20	19	405·8034	0·0011
21	20	405·9524	−0·0047
22	21	406·0971	0·0010
23	22	406·2140	−0·0051
24	23	406·3273	0·0015
25	24	406·4157	−0·0002

Table 7. Spectroscopic constants used in the fits.

	$(v = 0, K = 0)$†		$(v = 0, K = 1)$†¶		$(v_6 = 1, K = 1)$‡	
	$l(A^+)$§	$u(B^+)$§	$l(A^+)$§	$u(B^+)$§	$l(A^-)$§	$u(B^-)$§
$\bar{B}/\mathrm{cm}^{-1}$	0·2167083	0·2165735	0·217890	0·217693	$0{\cdot}2105_{62}$	$0{\cdot}2103_{05}$
$\bar{D}/10^{-6}\,\mathrm{cm}^{-1}$	2·0538	2·0380	2·043	1·953	$2{\cdot}5_{16}$	$2{\cdot}5_{41}$
$\bar{H}/10^{-12}\,\mathrm{cm}^{-1}$	−44·33‖	−47·14‖	−34·8	−34·8	0 (fix)	0 (fix)
$(B - C)/10^{-3}\,\mathrm{cm}^{-1}$	0‖	0‖	3·1697	3·044	$0{\cdot}7_{61}$	$0{\cdot}5_{37}$
$l/10^{-9}\,\mathrm{cm}^{-1}$	0‖	0‖	−77·3	−77·7	−70	−171
$\tilde{\nu}_0/\mathrm{cm}^{-1}$	0	0·65869	35·86236**	36·92275**	$399{\cdot}78_{65}$	$400{\cdot}75_{34}$*
			35·85919	36·92580		

† From [8], which uses also microwave data [3]. The constants were fixed in the fit.

‡ This work, uncertain digits are set as indices.

§ l is for the lower tunnelling level, u for the upper, the species Γ^{vb} of the vibrational state being given in parentheses.

‖ Set equal to zero in the fits for consistency of the model.

¶ These values were used for the calculation of ground state combination differences in table 5.

* Transition wavenumber from upper tunnelling level (measured band centre). The term value is 401·4121.

** Asymmetry doublet of the nearly symmetric rotor state.

The vibronic ground state of $(HF)_2$ is of A^+ species (Γ^{vb}), whereas the upper tunnelling component has B^+ species for the trans tunnelling path (see [29]). This would assign the 399·78 band to a transition from the tunnelling ground state A^+ and 400·75 to a transition from the upper tunnelling level. This is also consistent with the better root mean square deviations for this assignment shown in table 5. The significance of the different rms values for the two assignments is borderline,

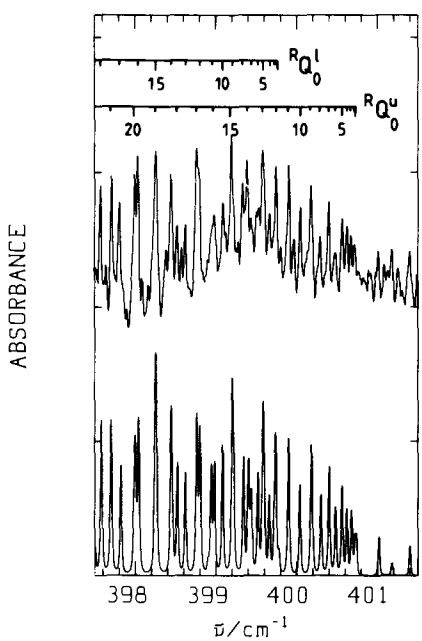

Figure 5. Detail of the experimental (upper trace) and simulated (lower trace) spectrum of $(HF)_2$ (see also figure 2 and text).

because the rotational constants of the two tunnelling components do not differ much at the level of our resolution. Higher resolution data would improve the significance, but are hardly necessary because of the symmetry assignment.

Excluding a perturbation (e.g. Coriolis coupling) which would invert the normal order of the $K_a K_c$-levels, all of the above results indicate a type C band polarization. Only the out of plane torsional transition is of type C. This assignment is to be compared further to the alternative, namely the $\nu_3(A')$ high frequency fundamental. This would result in a type B rotational band polarization (possibly a hybrid). There is also a second argument against this assignment. Assuming the trans tunnelling path, following Hougen and Ohashi [29] the ν_3 fundamental, which has A^+ vibrational symmetry Γ^v in the upper vibrational level (except tunnelling), would result in a transition from the *upper* tunnelling level in the vibrational ground state to the *lower* tunnelling level in the excited state and vice versa, similar to the symmetric HF stretching fundamental (see the left hand part of figure 7 of [29]). Excluding an inversion of the tunnelling levels in the excited vibrational state, which might, in principle, be caused by Fermi resonances and similar perturbations, the A^+ level should be lower in energy. Thus the $A^+(''') \rightarrow B^+(')$ vibronic transitions should occur at *high* frequency compared to $B^+(''') \rightarrow A^+(')$, if ν_3 were the correct assignment. The opposite behaviour is observed. The ν_3 assignment would thus appear to be excluded. The same kind of argument would also rule out any first overtone transition, which has $\Gamma^{v'} = A^+$, in particular the dimer valence stretching overtone.

The observed ordering of the two subband origins has a natural explanation if the assignment to the torsional fundamental is accepted. The difference of the two subband origins is here just equal to the increase of the tunnelling splitting, when going from the ground state with $K'' = 0$, $v_b = 0$ to the excited state with $K' = 1$, $v_b'' = 1$.

Table 8 summarizes the tunnelling splittings for different fundamentals from the work of Pine *et al.* [9] and the present investigation. It is seen that both rotational excitation by $\Delta K = 1$ and vibrational excitation of the torsion lead to an increase of the tunnelling splitting by about a factor of 1·5. In contrast to this, HF vibrational stretching excitation gives a *decrease* of the tunnelling splitting. Both effects can be understood with simple models. In particular, the increase of tunnelling rate with torsional excitation indicates some contribution of the out of plane motion to the interconversion of conformers. This contribution is expected but now found to be still relatively small, which would seem to justify the decision of Hougen and Ohashi to concentrate on planar tunnelling motion [29]. The relatively small tunnelling splitting of the excited state is also evidence against all assignments involving some excitation of the large amplitude bending motion, assuming that this can be associated with both the tunnelling coordinate and the predicted low frequency bending

Table 8. $(HF)_2$ tunnelling splittings $\Delta\nu$ for three fundamentals.

	$\Delta\nu$/GHz			
K	$v = 0$	$v_1 = 1$	$v_2 = 1$	$v_6 = 1$
0	19·747	6·461	6·998	—
1	31·911	10·488	10·225	$48{\cdot}7_7$
Reference	[9, 3]	[9]	[9]	This work

fundamental. Together with the symmetry assignment, this would rule out all possible assignments of the observed band to an overtone or combination tone.

The decrease of B_{vk} with torsional excitation is expected because of the weaker and thus longer hydrogen bond in excited torsional states. Related decreases have been found in HCN···HF [35] and rare gas ···HF complexes [36]. In $(HF)_2$ $(B'' - B')$ is a factor of three larger than for (HCN···HF). Another interesting observation is the decrease of the asymmetry splitting (by a factor of 6) in the $K_a = 1$ state upon torsional excitation. The value of $(B - C)$ is comparable to that of the quasilinear molecular HNCS [38]. A question arises concerning the intensity of the $K = 2 \leftarrow 1$ subband, which in an ordinary molecule should be about as intense as $K = 1 \leftarrow 0$. It is obvious from figure 1 that to the high wavenumber side there are only rather weak bands. This might be explained by a decrease of intensity of $K = 2 \leftarrow 1$ or by a spreading of the intensity over a wider range. Interestingly rather intense subbands occur to the *low* wavenumber side of the 400 cm^{-1} system.

3.4. *Further subbands and possible assignments*

Two moderately strong subbands can be assigned near 380 cm^{-1}. The analysis of these bands is less straightforward than for the 400 cm^{-1} region. Firstly the signal to noise ratio is somewhat poorer to low wavenumbers for the Cu/Ge detector used here. This causes difficulties for the analysis of the high Q-branch transitions and for the P-branch. Secondly, the R-branch overlaps considerably with the 400 cm^{-1} bands, resulting in a very congested spectrum. The difficulty is amplified by apparent perturbations for $J > 30$ in the 400 cm^{-1} band. The Q-branches are, however, rather clear and figure 6 shows a detail of the structure. A list of assigned transitions is presented in table 9. There is no evidence for asymmetry splitting. Spin statistical intensity alternations are visible, but not very compelling. Due to the lack of adequate ground state combination differences, the ground state of the transition cannot be established beyond doubt. Three possible assignments are: (i) The $K = 0 \leftarrow 1$ transition of the torsion; (ii) the $K = 0 \leftarrow 1$ transition of the in plane bending; (iii) the $K = 1 \leftarrow 0$ of the in plane bending vibration. Other assignments,

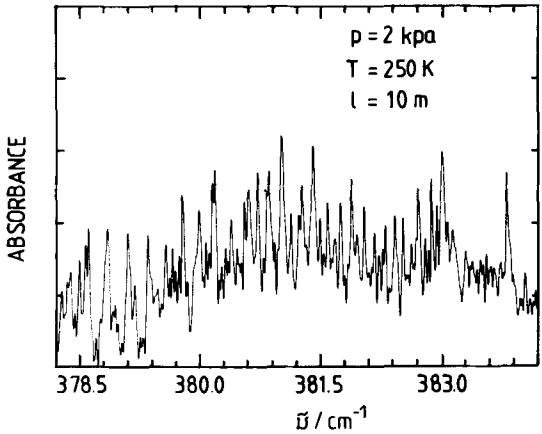

Figure 6. Detail of the subband near 380 cm^{-1} (see text, resolution = 0·02 cm^{-1} FWHM, $p = 2$ kPa, $T = 250$ K, $l = 10$ m).

Table 9. Assigned Q-branch transitions of the subbands near 380 cm^{-1}.
(*a*) Upper tunnelling component (ν^0_{sub} = 383·34 cm^{-1}).

$J' = J''$	Wavenumber/cm^{-1} $\tilde{\nu}_{exp}$	$(\tilde{\nu}_{exp} - \tilde{\nu}_{calc})$
8	383·1399	0·0004
9	383·0881	0·0010
10	383·0238	−0·0046
11	382·9613	−0·0020
12	382·8901	−0·0014
13	382·8132	0·0004
14	382·7274	0·0003
15	382·6385	0·0044
16	382·5321	−0·0014
17	382·4323	0·0071
18	382·3094	0·0006
19	382·1871	0·0030
20	382·0492	−0·0016
21	381·9037	−0·0048
22	381·7610	0·0041
23	381·5912	−0·0044
24	381·4244	0·0000
25	381·2392	−0·0035
27	380·8483	0·0018
29	380·4003	−0·0034
30	380·1676	0·0039

(*b*) Lower tunnelling component ($\tilde{\nu}^0_{sub}$ = 382·028 cm^{-1}).

$J' = J''$	Wavenumber/cm^{-1} $\tilde{\nu}_{exp}$	$(\tilde{\nu}_{exp} - \tilde{\nu}_{calc})$
7	381·7610	−0·0001
8	381·6938	0·0093
9	381·5912	−0·0071
10	381·4973	−0·0051
11	381·3940	−0·0029
12	381·2856	0·0040
13	(381·142)	−0·0145
14	(381·002)	−0·0196
15	380·8795	0·0026
16	(380·733)	0·0107
17	380·5595	0·0018
19	380·1968	−0·0018
20	380·0064	0·0025
21	379·7912	−0·0079
22	379·5848	0·0008
23	379·3634	0·0047
24	(379·110)	−0·0130
26	378·6193	−0·0009

such as vibrational hot band transitions are less likely. Each of the above assignments would have interesting implications. The first assignment would assume that the energy of the $K = 0$, $v = 1$ state is higher than of $K = 1$, $v = 1$. This could result from Coriolis interaction with higher states as has been observed for HNCS [38]. One would also have to assume an inversion of the tunnelling doublet. The second assignment would imply a change of the expected intensity distributions for the $K = 0 \leftarrow 1$ and $K = 1 \leftarrow 0$ transitions, for example due to a B/C Coriolis coupling [39]. This assignment would also imply a very small tunnelling splitting of $0{\cdot}26\,\mathrm{cm}^{-1}$ in the excited state. The third assignment is very attractive because it is consistent with the chemical intuition that the torsion and the in plane bending vibration are really a pair of nearly degenerate vibrations resulting from the zero order picture of a linear F–H···F molecule with a degenerate bending vibration. However, all *ab initio* calculations predict the in plane bending vibration to occur at *higher* frequency than the torsion. Thus the vibrational assignment must remain open, at present.

The rotational assignment is also still somewhat uncertain. A shift of the J assignment by (± 1) unit gives fits of practically identical quality as the assignment given in table 9. Larger shifts give systematically poorer root mean square deviations. The constants arising from the more probable assignments are summarized in table 10. The change of rotational constants for this state is about a factor of 2 smaller than for the $400\ \mathrm{cm}^{-1}$ level.

4. Conclusions and outlook

It has been possible to detect and assign parts of the weak and highly complex rovibrational spectrum of the hydrogen fluoride dimer in the far infrared. A subsystem near $400\,\mathrm{cm}^{-1}$ can be identified with a high degree of confidence as being due to the tunnelling levels of the $K = 1 \leftarrow 0$ transition of the torsional (A'') fundamental, which would then normally fall around $320\,\mathrm{cm}^{-1}$. We may summarize the main arguments in favour of this assignment:

Table 10. Constants obtained from the fits of the $380\,\mathrm{cm}^{-1}$ bands ($\Delta X = X' - X''$).

	(A)		
	a	*b*	*c*
$\tilde{\nu}_{\mathrm{sub}}/\mathrm{cm}^{-1}$	$383{\cdot}34_{45}$	$383{\cdot}37_{75}$	$383{\cdot}31_{00}$
$\Delta B_{\mathrm{eff}}/\mathrm{cm}^{-1}$†	$-0{\cdot}0027_{96}$	$-0{\cdot}0025_{46}$	$-0{\cdot}0030_{77}$
$\Delta D_{\mathrm{eff}}/10^{-6}\,\mathrm{cm}^{-1}$‡	$0{\cdot}6_{7}$	$0{\cdot}7_{0}$	$0{\cdot}6_{1}$
rms/cm^{-1}	0·0032	0·0038	0·0031
	(B)		
	a	*b*	*c*
$\tilde{\nu}_{\mathrm{sub}}/\mathrm{cm}^{-1}$	$382{\cdot}02_{85}$	$382{\cdot}08_{07}$	$381{\cdot}97_{50}$
$\Delta B_{\mathrm{eff}}/\mathrm{cm}^{-1}$	$-0{\cdot}0047_{65}$	$-0{\cdot}0043_{49}$	$-0{\cdot}0052_{36}$
$\Delta D_{\mathrm{eff}}/10^{-6}\,\mathrm{cm}^{-1}$	$0{\cdot}04_{6}$	$0{\cdot}2_{2}$	$-0{\cdot}2_{1}$
rms/cm^{-1}	0·0046	0·0049	0·0056

† $B_{\mathrm{eff}} = \bar{B}_{\mathrm{vk}} \pm \delta_{\mathrm{kl}}(B - C)/4$.
‡ $D_{\mathrm{eff}} = D_{\mathrm{vk}} \pm \delta_{\mathrm{kl}}\, l_{\mathrm{vk}}/2$.

(i) From *ab initio* calculations the band is expected to belong to one of the two higher frequency fundamentals of the low frequency modes.

(ii) The symmetry assignment of the tunnelling components by means of nuclear spin statistics defines the vibrational symmetry of upper and lower tunnelling levels.

(iii) The ground state of the transition is shown to be the vibrational ground state by combination differences of assigned rotational lines and known data from I.R. and microwave spectroscopy.

(iv) Overtone and combination transitions of the low frequency bending are excluded because of the modest increase in the tunnelling splitting. The overtone of the hydrogen bond (F–F stretching) vibration is excluded because of its symmetry.

(v) One observes no K-type asymmetry splitting, which is consistent with a $K = 1 \leftarrow 0$ transition.

Although one might raise objections against any single argument, for instance the symmetry assignments depend somewhat upon dynamical assumptions made in the group theoretical analysis of the tunnelling process [29], the ensemble of reasons renders the assignment rather compelling. The assignment of a second observed subband near $380\,\mathrm{cm}^{-1}$ is still uncertain. More complete interpretation will be possible when further low frequency modes are observed and analysed. Such work is in progress in our laboratory.

E. Peyer contributed importantly to the construction of the long path sample cell with temperature control. Discussions with H. Bürger, L. Halonen, H. Hollenstein and M. Suhm are acknowledged as well as financial support of our work by the Schweizerischer Nationalfonds and the Schweizerischer Schulrat.

References

[1] PIMENTEL, G. C., and MCCLELLAN, A. L., 1960, *The Hydrogen Bond* (Freeman). SCHUSTER, R. (editor), 1984, *Hydrogen Bonds* (Top. Curr. Chem., Vol. 120).

[2] RENSBERGER, K. J., COPELAND, R. A., ROBINSON, J. M., and CRIM, F. F., 1985, *J. chem. Phys.*, **83**, 1132.

[3] DYKE, T. R., HOWARD, B. J., and KLEMPERER, W., 1971, *J. chem. Phys.*, **56**, 2442.

[4] HOWARD, B. J., DYKE, T. R., and KLEMPERER, W., 1984, *J. chem. Phys.*, **81**, 5417.

[5] GUTOWSKY, H. S., CHUANG, C., KEEN, J. D., KLOTS, T. D., and EMILSSON, T., 1985, *J. chem. Phys.*, **83**, 2070.

[6] LAFFERTY, W. J., SUENRAM, R. D., and LOVAS, F. J., 1987, *J. molec. Spectrosc.*, **123**, 434.

[7] REICHERT, U. V., and HARTMANN, H., 1972, *Z. Naturforsch* (*a*), **27**, 983.

[8] PINE, A. S., LAFFERTY, W. J., 1983, *J. chem. Phys.*, **78**, 2154.

[9] PINE, A. S., LAFFERTY, W. J., and HOWARD, B. J., 1984, *J. chem. Phys.*, **81**, 2939.

[10] PUTTKAMER, K. V., and QUACK, M., 1985, *Chimia*, **39**, 358.

[11] PUTTKAMER, K. V., and QUACK, M., 1986, *Faraday Discuss. chem. Soc.*, **82**, 377, and to be published.

[12] SMITH, D. F., 1968, *J. chem. Phys.*, **48**, 1429.

[13] HUONG, P. V., and COUZI, M., 1969, *J. Chim. phys.*, **66**, 1309.

[14] REDINGTON, D. L., and HAMILL, D. F., 1984, *J. chem. Phys.*, **80**, 2446. KLEIN, M. L., MCDONALD, I. R., and O'SHEA, S. F., 1978, *J. chem. Phys.*, **69**, 63. KLEIN, M. L., and MCDONALD, I. R., 1979, *J. chem. Phys.*, **71**, 298.

[15] ANDREWS, L., BONDYBEY, V. E., and ENGLISH, J. H., 1984, *J. chem. Phys.*, **81**, 3452.

[16] HUNT, R. D., and ANDREWS, L., 1985, *J. chem. Phys.*, **82**, 4442.
[17] ANDREWS, L., and JOHNSON, G. L., 1983, *Chem. Phys. Lett.*, **62**, 875.
[18] FRANCK, E. U., and MEYER, F., 1959, *Z. Elektrochem.*, **63**, 571.
[19] FRISCH, M. J., DEL BENE, J. E., BINKLEY, J. S., and SCHAEFER, H. F., 1986, *J. chem. Phys.*, **84**, 2279.
[20] GAW, J. F., YAMAGUCHI, Y., VINCENT, M. A., and SCHAEFER, H. F., 1984, *J. Am. chem. Soc.*, **106**, 3133.
[21] CURTISS, L. A., and POPLE, J. A., 1976, *J. molec. Spectrosc.*, **61**, 1.
[22] KOLLMAN, P. A., and ALLEN, L. C., 1970, *J. chem. Phys.*, **52**, 5085.
[23] BARTON, A. E., and HOWARD, B. J., 1982, *Faraday Discuss. chem. Soc.*, **73**, 45, 122.
[24] REED, A. E., WEINHOLD, F., CURTISS, L. A., and POCHATKO, D. J., 1986, *J. chem. Phys.*, **84**, 5687.
[25] LONGUET-HIGGINS, H. C., 1963, *Molec. Phys.*, **6**, 445.
[26] QUACK, M., 1977, *Molec. Phys.*, **34**, 477.
[27] BUNKER, P. R., 1979, *Molecular Symmetry and Spectroscopy* (Academic Press).
[28] MILLS, I. M., 1984, *J. phys. Chem.*, **88**, 532.
[29] HOUGEN, J. T., and OHASHI, N., 1985, *J. molec. Spectrosc.*, **109**, 134. DALTON, B. J., and NICHOLSON, P. D., 1975, *Int. J. quant. Chem.*, **9**, 325.
[30] HALBERSTADT, N., BRÉCHIGNAC, PH., BESWICK, J. A., and SHAPIRO, M., 1986, *J. chem. Phys.*, **84**, 170.
[31] ROTHSCHILD, W. G., 1964, *J. opt. Soc. Am.*, **54**, 20.
[32] HERZBERG, G., 1945, *Molecular Spectra and Molecular Structure*, Vol. II (van Nostrand).
[33] PUTTKAMER, K. v., and QUACK, M. (to be published).
[34] MARQUARDT, D. W., 1963, *J. Soc. ind. appl. Math.*, **11**, 431.
[35] WOFFORD, B. A., BEVAN, J. W., OLSON, W. B., and LAFFERTY, W. J., 1986, *Chem. Phys. Lett.*, **124**, 579.
[36] LOVEJOY, CHR. M., SCHUDER, M. D., and NESBITT, D. J., 1986, *J. chem. Phys.*, **85**, 4890.
[37] FRASER, G. T., and PINE, A. S., 1986, *J. chem. Phys.*, **85**, 2502.
[38] YAMADA, K., and WINNEWISSER, M., 1977, *J. molec. Spectrosc.*, **64**, 401.
[39] HOLLENSTEIN, H., 1980, *Molec. Phys.*, **39**, 1013.
[40] COLE, A. R. H., 1977, *Tables of Wavenumbers* (Pergamon Press). 1971, *CRC Handbook of Lasers* (CRC Press).
[41] MICHAEL, D. W., DYKSTRA, C. E., and LISY, J. M., 1984, *J. chem. Phys.*, **81**, 5998.